Thai Environmental Engineering Journal Vol. 34 No. 3 (2020) : 1-9
www.eeat.or.th

Investigation of Contaminated Soil Formed at River Bank Located Downstream of Mines

Sachi A. Wakasa[1*], Vladan Marincović[2], Tomomi Takeda[3], Junichi Kurihara[4], Lidja Đurđevac Ignjatović[2], Tamara Urosević[2] and Renata Kovacević[2]

[1*]Institute of Regional Innovation, Hirosaki University, Aomori 030-0813, Japan

[2]Mining and Metallurgy Institute Bor, Serbia

[3]Japan Space Systems, Japan

[4]Faculty of Science, Hokkaido University, Japan

[*]E-mail : wakasa@hirosaki-u.ac.jp

Abstract

The purpose of this study is to find out how polluted a riverbank located downstream of the mines where has been excavated for more than 100 years in Serbia. A field survey was conducted, and ground surface sediments from rivers were collected, sediment thickness and density were measured, and soil pits were excavated. The inside of those pits were observed and the sediment samples were collected. The surface sediments collected were subjected to mineral identification using XRD, and the sediments collected from the pits were subjected to chemical analysis. On the other hand, a high-accuracy ortho-image was created by using UAV to acquire visible images with 60% or more of each other overlapping and by acquiring position information using high-accuracy GPS. From this image, the area of the riverbank was measured using GIS software. In addition, a camera capable of acquiring hyperspectral images was installed in the UAV to acquire hyperspectral images. From the obtained image analysis results, it became clear that pollutants from the mine were distributed on most of the surface of this riverbank. The conclusion of this study is that there is a high possibility that the waste material from the mine had been accumulated at the riverbank that was the subject of this study, and the area was occupied with 96,000 m^2, the volume is 78,600 m^3 in volume and 152,400 t in weight.

Keywords : contaminated soil; heavy metal; field survey; UAV; jarosite

Introduction

Contaminated soil is produced in mines and under geological conditions. Especially in the vicinity of the mine, the pollutants are suddenly discharged and diffused from the start of excavation, which causes serious environmental pollution. The polluted soil discharged by mining moves on the ground surface by the force of water and wind like other debris. It is known that contaminated soil carried by river water behaves similarly to other debris [1]. However, without knowing the actual status of the deposited pollutants, it is not possible to discuss environmental pollution status, future diffusion potential, environmental impact, and measures to improve them. Therefore, in this study, we will report the results of field surveys and environmental surveys using UAVs for the current state of sediments in rivers that have been transported and deposited by river water around the mine.

Study Area

Bor and its surroundings in eastern Serbia are well known for copper deposits, which are among the largest in Europe (**Figure 1**). Around these deposits, many current and historical copper mines were developed since 1903. Our study area is the floodplain of a river located downstream of the Bor mine. The Bor mine has been mined upstream of the Bor and Krivelj rivers and started in 1903 and 1979, respectively. They are called Old-Bor mine and Veliki Krivelj mine (**Figure 1b**). The study area is a riverbank formed at the confluence of these Bor and Krivelj rivers (**Figure 2a, c**).

Underground mining started at Old-Bor mine in 1903 and open pit excavation began in 1923. Drilling was continued until 1993. During that period, mine waste was directly discharged into rivers until 1933, after that, overburden, low-grade ore, and tailing were deposited around the mine. At Veliki Krivelj mine, excavation of the open pit started in 1979, and overburden, low grade ore and tailing are deposited around the open pit. Direct disposal to the river at the beginning of excavation at Old-Bor mine is a problem. Regarding the tailings, the dam constructed as a sedimentation site is the dam that built up the tailings themselves, and is not fixed or covered (**Figure 2b**). It is not difficult to imagine how these will behave due to rainwater or river runoff.

In the study area, rivers with debris are deposited on the Bor river and Krivelj river in front of the confluence, and after the confluence, a wider riverbank is formed (**Figure 2**). Figure 2a shows the riverbank formed along the Bor river, and Figure 2c shows the confluence of the Bor and Krivelj rivers.

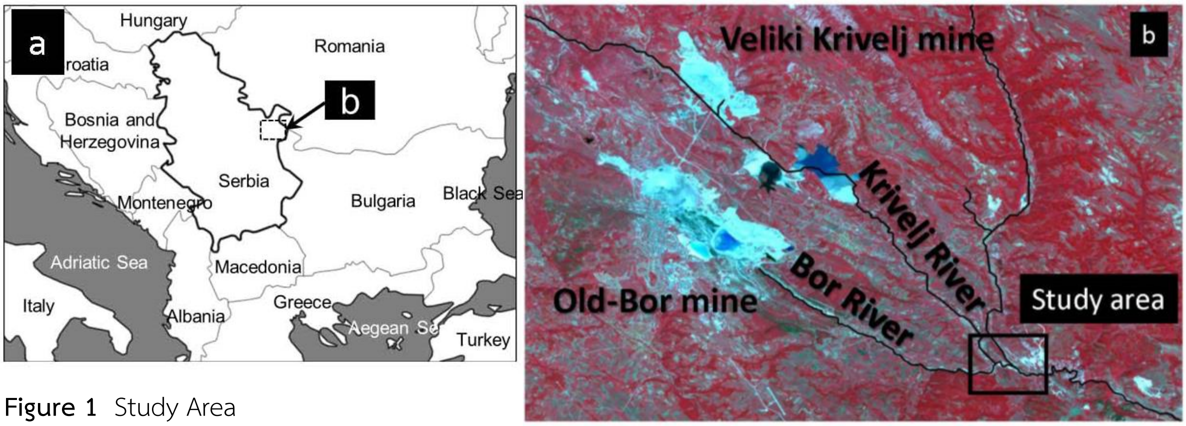

Figure 1 Study Area

Figure 2 The Study Area
(a) Bor River Riverbank (b) Tailings dam of Old-Bor Mine and (c) confluence of the Bor and Krivelj Rivers

Methodology

To clarify the current condition of the target river basin, we conducted a field survey, analyzed the collected samples in the laboratory, and analyzed the images acquired by UAV.

In the field survey, surface material was sampled, then the mineral composition of the samples was investigated using X-ray diffraction analysis (XRD). Riverbanks sediments developed along each river were excavated, and sedimentary facies of the pits were observed. The sediment samples were also collected from the excavated pits. The sediment samples were analyzed for chemical content by ICP-MS and FAAS. The depths of sediments were investigated using a cone penetration test. The density was obtained by measuring the weight of the ground surface sample collected in a fixed form on the spot.

Two types of images were acquired using UAV. One is a set of visible images in which adjacent places overlap to create a high-precision digital topographic map. The set was taken using GoPro camera mounted on Phamtom3. The other set is hyperspectral images for classifying the reflection properties of surface materials. A total of 46 hyperspectral images were acquired every 10 nm in the range of 600-1050 nm. Since it was necessary to change the exposure time during shooting, the shouting was carried out twice and the images were gotten a total of 92. An LCTF camera was used for the image acquisition [2]. The aerial photography carried out with the LCTF camera mounted on the UAV was carried out by requesting a specialized UAV pilot on 6th September, 2018.

To create a high-precision topographic map, the acquired photographs are made into point clouds using photo composition software (PhotoScan, Agisoft). The position information was also acquired by UAV, but it was corrected by the ground control point (GCP) acquired by high-precision GPS locally (Trimble R4). After correction, the area of the riverbank was measured from the created ortho image using ArcGIS software (ESRI).

The photographs taken by the LCTF camera were corrected geometrically for 46 images of each set, then normalized using grey mat corrected in laboratory. Finally, the two set were georeferenced and merged. From the merged image, a spectral curve can be obtained for each pixel. However, it was difficult to correlate with the spectrum curve obtained by the existing spectrometer. On the other hands, there was a difference in the spectrum for each pixel, and it was possible to perform spatial analysis on the same image. Therefore, supervised data was acquired from the obtained image, and supervised analyses was performed (Here, the SAM method was adopted).

Results and Discussions

XRD of surface samples revealed that it contains jarosite, which is often found around mines where pyrite is often produced. Therefore, as shown in **Figure 3**, the quantity ratio of jarosite at the sampling point is shown by circles: large content: L for red, medium content: M for green, and small content: S for blue. Jarosite is a secondary mineral of iron oxide minerals and is a recrystallized product of mine waste dissolved in water [3]. In addition, since water used for crystallization is around pH2 [3], it indicates that acidic water is present in the environment where jarosite is produced.

Soil pits were dug on the left bank of the Bor and the right bank of the Krivelj. **Figure 4** shows each of the soil faces and the concentrations of copper, lead, arsenic, and manganese measured by ICP-MS and iron and sulfur concentrations measured by FAAS for each sedimentary structure. There are six sedimentary layers in the pit of the Bor river, and alluvial deposits were observed beneath them. The concentration of alluvium is lowest. The concentration of the second layer of the Bor river bank is missing and not shown. In the sixth layer at a depth of 62-120 cm, sub-angular gravels with a maximum diameter of 20 cm were observed, and the concentrations of copper, iron and sulfur were high at 1,900 ppm, 17%, and 27% respectively. Lead and arsenic had the highest concentrations in the uppermost layer, 220 ppm and 240 ppm, respectively. Manganese concentration was highest in the second layer. In the uppermost layer, copper and iron were also generally high in concentration and were 550 ppm and 4%, respectively.

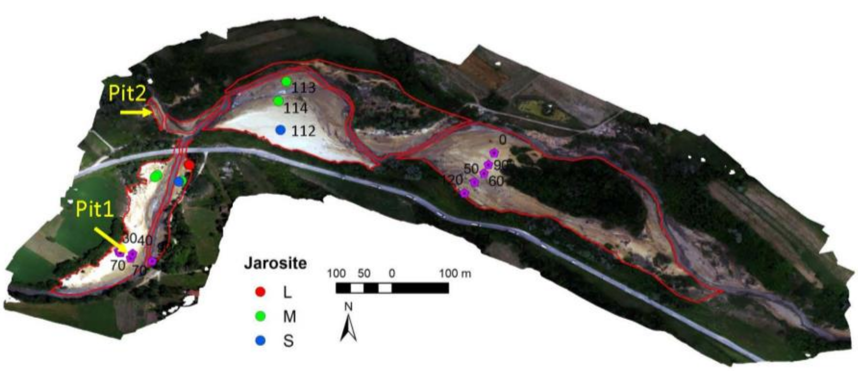

Figure 3 Field survey data on the orthoimages created in this study

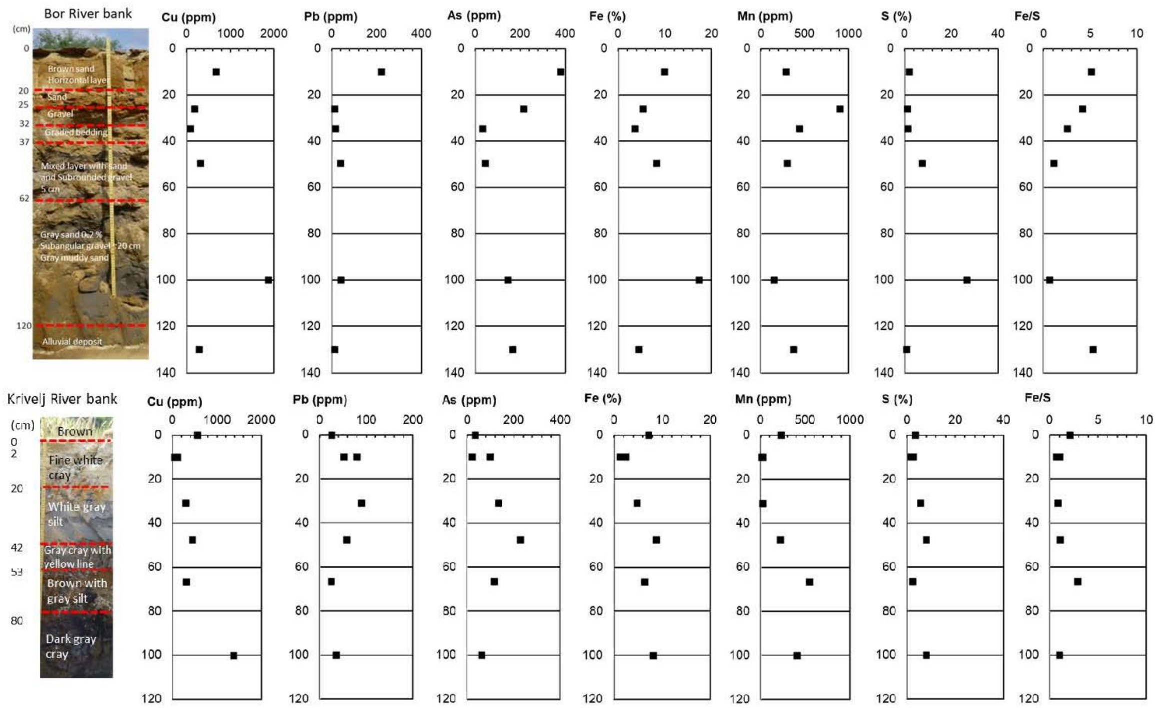

Figure 4 Soil faces and concentrations of copper, lead, arsenic, and iron of each layer of pits

As mentioned above, at Old-Bor mine, for about 30 years after the start of mining in 1903, mine waste was directly discharged to rivers. The 20 cm-sized gravel found at the sixth layer of the Bor riverbank deposit is considered to be waste at that time. This can also be explained by the extremely high concentration of copper, iron and sulfur in the bottom layer. It can be estimated from the mining record of the Old-Bor mine that the copper concentration was 6% for the first 30 years [4]. It is presumed that the gravel with such a large diameter had flowed down since the early 1933, as waste was deposited on dams and sedimentation sites. On the other hand, in the upper deposit, the grain size of sand to silt is accumulated in layers, and the grade structure is seen in the fourth layer. It can be inferred that these deposits flowed down after the tailing dam was formed and when the dam wall collapsed due to a flood. The depth profiles of the concentrations except manganese and sulfur are similar. It can be inferred that this sediment does not move much physically from the time of deposition and represents the situation at the time of deposition. Manganese and sulfur are easier to move than iron. Especially in the 1st to 3rd layers, the amount of sulfur is relatively small, which suggests that the upper layer is being oxidized. Further, the fourth and fifth layers had a high sulfur concentration, and their ratios to iron were 1.1 and 0.7. In other words, the area around this depth is in an anaerobic state, indicating that the oxidation of pyrite has not progressed. Probably indicates that the area around this layer is the water table.

Six sedimentary layers were also observed in the Krivelj river pit, but the structure of the sediments was very different from that of the Bor river. In addition, due to the water table, it was not possible to dig into a layer below the bottom layer. The pit deposits on the Krivelj River were fine, mostly clay to silt size. Strong elasticity and plasticity were observed in the dark gray clay layer at the bottom. Even in the Krivelj River pit, the concentration of copper in the bottom layer was the highest, at 1,400 ppm. On the other hand, the concentrations of iron and arsenic were high in the middle white gray silt layer, 8.9% and 230 ppm, respectively. Manganese and sulfur concentrations did not differ from those found in Bor. The Fe/S ratio was 1 or less than 1 in most layers. Only in the layer of 53 to 80 cm, the Fe / S ratio was 2.9. The color of this layer is brown, consistent with the oxidation and sulfur elution that would have occurred.

The sediments of the Krivelj riverbank are even finer. This is convincing evidence that the tailings produced during excavation and beneficiation after 1979, when technological innovation has passed, may have flowed down. The investigation of these particle sizes was only visual and could not be accurately measured. The difference in concentration in each layer may be interpreted by comparing it with the drilling record. However, the behavior of heavy metals in soil must also be considered, and this study has not considered it. I would like to make it a future issue. Both Bor riverbank and Krivelj riverbank have six sedimentary layers. In order to interpret this, it is necessary to carry out more detailed topographical survey. On the other hand, it was estimated that the Bor riverbank deposits were brown and had less sulfur than when they were deposited. It can be estimated that sufficient time has elapsed for oxidation. On the other hand, in the Krivelj riverbank, white and gray deposits are present, suggesting that they have not yet been oxidized. Bor deposits should be from over 100 years old and Krivelj deposits from the last 40 years. What is the reason for this difference in deposition period and the same number of layers? There are several possible reasons for this. (1) During the first 70 years, deposits from Old-Bor mine were deposited on the Bor river bank. As a result, the riverbed of the Krivelj river was lowered, and the environment became prone to deposits in the Krivelj riverbank. (2) Since the Krivelj River has a larger catchment area than one of Bor river, sediments are more likely to collect. (3) Veliki Krivelj mine has undergone technological innovation and has undergone large-scale construction, so the amount of sediment has increased rapidly, and a large amount of sediment has come to flow suddenly. (4) Lots of bedding is visible in the sediments of the Bor riverbenk, and there may be other bedding that cannot be distinguished in this observation. In any case, since all the layers contain chemical substances that are considered to be of mine origin, it can be inferred that all of these deposits were mine waste.

As observed in the two soil pits, the deposit thickness was 120 cm and deeper than 100 cm, respectively. In addition, the thickness of sediments in the riverbank was examined by a portable corn penetration tester. The survey points are the purple hexagonal points shown in **Figure 3**, and the results are the numbers written at each point. The depth near the river channel was deep, and the one far was shallow. The average of the Bor riverbank was 70 cm, and the one of the Krivelj and after junction riverbank was 84 cm. Overall, the average sediment depth was 76 cm. On the other hand, the density of surface sediments was also measured in the riverbank of Bor river, Krivelj river, and after the junction. Their values were 1.76 g/cm^3, 1.76 g/cm^3, and 1.97 g/cm^3, respectively.

Figure 3 shows the ortho image created from the visible images. This image was position corrected with 15 GCP points measured by precision GPS sensor. In this study, the area of riverbank sediment was estimated from this ortho image. Polygons were created with the area surrounded by the red line in the figure as riverbank sediment, and the area of the polygon was calculated. As a result, the total area of riverbank sediments in this area was estimated to be 96,000 m^2.

The volume of riverbank sediment was calculated based on the sediment density, the average depth and area of the sediment from the field surveys in this study. The volume of the riverbank was calculated simply by dividing it into the Bor riverbank, the Krivelj riverbank, and the riverbank after confluence. The result was calculated as 18,400 t, 2,600 t and 131,400 t, respectively. Therefore, the total was 152,400 t. The volume was 78,600 m^3. In other words, if it is necessary to cover contaminated soil for environmental protection, it is necessary to work to cover the ground surface of 96,000 m^2 or more. Also, if contaminated soil is to be removed, 152,400 t of soil must be transported and deposited.

Obtained 92 hyperspectral images was position and color corrected. As the result, spectral data of 600 to 1050 nm was obtained for each pixel. The obtained spectrum data from the images and the ground truth samples are shown in the **Figure 5**. For the ground truth samples, it was assumed that the stronger the jarosite peak intensity during XRD, the higher the amount of jarosite. The medium amount is Jarosite M, and the small amount is Jarosite S. The spectral curves of the ground truth samples in Figure. 5 were the result of analyzing them in the laboratory using portable spectroradiometer (FieldSpec). The reference values for jarosite were obtained from the USGS spectral library [5], and the values were normalized and shown in **Figure 5**. Among the reflection characteristics of jarosite, the absorption band seen near 900 nm is one of its characteristics [6]. The spectral characteristics of the ground truth sample show which absorption bands are slightly visible. The spectrum curve obtained from the hyperspectral image is not clear, although it can be seen depending on the appearance. It is necessary to conduct more statistical analysis in the future, but in this study, we will limit the interpretation to this point. Therefore, the spatial distribution analysis of the by selecting the supervised data from the own image (**Figure 6**). The supervised data was selected by field survey to determine the ROI range of trees, roads and rivers. For Jarosite M and Jarosite S, ROI was created around the point where each ground truth sample was collected (area surrounded by squares in **Figure 6**). Spectral Angle Mapper (SAM) method was used for supervised classification.

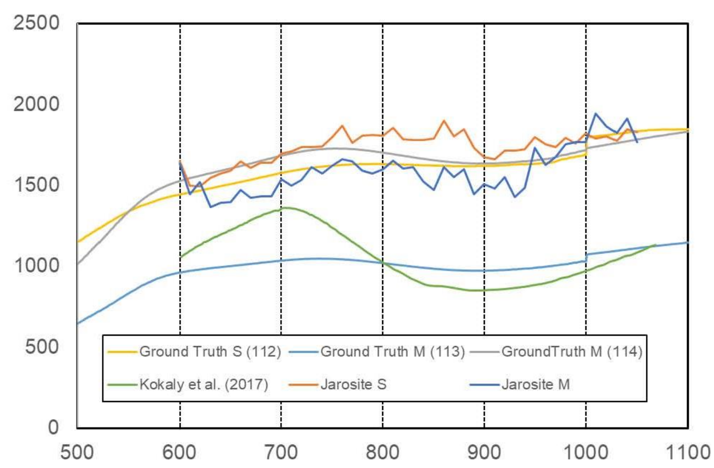

Figure 5 Spectral features obtained from hyperspectral image and ground truth samples

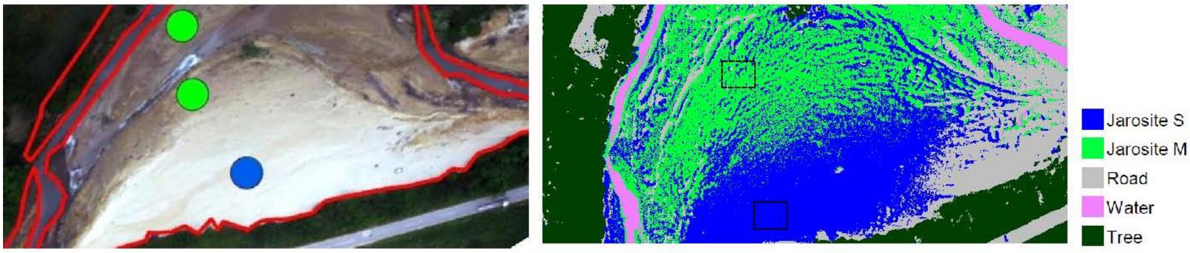

Figure 6 Spatial classification analysis result. The left side is the relevant part of the analysis in Figure 3

Spatial distribution analysis results show that components with the same spectral characteristics as roads also appeared on the surface of the sediment, and it is hard to say that it was completely successful. However, the classification of trees and water is well done, and the classification of Jarosite S and Jarosite M brings interesting results. It is regrettable that many roads have been included, but the control ratio in the Figure 6 for each component is shown in **Table 1**. From the distribution characteristics of Jarosite M and Jarosite S, the distribution of Jarosite M tends to be closer to the river. This may suggest that the frequency of inundation affects the oxidation of surface materials. Also, it seems that Jarosite M covers Jarosite S. This might indicate that the more recently deposited material contained more M, or that the sheet flood flow made the surface material more oxidized. Furthermore, the planar structure of the deposit can also be estimated from this figure. In the area close to the river channel, a lump-like, band-like, and sedimentary structure along the flow channel is seen, whereas in the area far from the river channel, it seems to have a granular and individual distribution. On the other hand, what does the surface sediment classified as the road represent? Usually, road materials are used in the surrounding area, so it is not so strange that the same materials come out. Also, in Figure. 6, it seems to be distributed far from the river channel, further below the jarosites M and S, and at the most downstream of the meandering part of the river. This may be due to the fact that sediment oxidation has not occurred in this area or the acid stream flow has not reached this far. In any case, the result of this analysis of hyperspectral images is that the sediment containing jarosite covers most of the riverbank. Whether this is changing over time will be answered by reacquiring the image at a later time. Since it is a UAV-based research, it may be a relatively easy future, but I look forward to future research.

Table 1 Distribution ratio of each component in Fig. 6

Image Class	Samples	Percent
Jarosite S	56,132	32.0
Jarosite M	48,945	27.9
Road	31,130	17.7
Water	5,371	3.10
Tree	33,826	19.3
Total	**175,404**	**100**

Conclusion

In this study, we used geoscience techniques and UAV techniques to investigate the state of the sediment in a riverbank located downstream of a mine. It was found that the target deposit contained jarosite, a secondary iron oxide mineral. In addition, inspection of the sediment structure of the two soil pits and chemical analysis of the sediment samples confirmed the presence of mine waste deposits in the riverbank. Besides, we estimated the area and amount of contaminated sediment containing these, and obtained the necessary numbers to remove these contaminations. In addition, the hyperspectral image obtained by UAV confirmed that the pollutant was spreading over the entire ground surface.

Acknowledgement

This research was partially supported by the Japan Science and Technology Agency (JST) and the Japan International Cooperation Agency (JICA) through Science and Technology Research Partnership for Sustainable Development (SATREPS). This work was also supported by JSPS KAKENHI Grant Number 17K17613.

Reference

[1] Macklin, M.G., Brewer, P.A., Hudson-Edwards, K.A., Bird, G., Coulthard, T.J., Dennis, I.A., Lechler, P.J., Miller, J.R., and Turner, J.N. 2006. A geomorphological approach to the management of rivers contaminated by metal mining. Geomorphology. 79: 423-447.

[2] Kurihara, J., Ishida, T., and Takahashi, Y. Unmanned Aerial Vehicle (UAV)-Based Hyperspectral Imaging System for Precision Agriculture and Forest Management. In: Avtar, R. and Watanabe, T. Unmanned Aerial Vehicle: Applications in Agriculture and Environment, Springer, 2020; 25-38.

[3] Nordstrom, D.K., Alpers, C.N. Geochemistry of Acid Mine Waters. In: Plumlee, G.S. and Logsdon, M.J. eds., Chap. 6, The Environmental Geochemistry of Mineral Deposits, Rev. Econ. Geol. V. 6A, Soc. Econ. Geol. Inc., Litteleton, CO, 1999.

[4] Japan International Cooperation Agency Economic Development Department (JICA report), 2008. Actual situation and problems of mining activities: Mining Promotion Master Plan Survey Final Report of the Republic of Serbia. 70-121.

[5] Kokaly, R.F., Clark, R.N., Swayze, G.A., Livo, K.E., Hoefen, T.M., Pearson, N.C., Wise, R.A., Benzel, W.M., Lowers, H.A., Driscoll, R.L., Klein, A.J., 2017, USGS Spectral Library Version 7: U.S. Geological Survey Data Series 1035, 61 p., https://doi.org/10.3133/ds1035.

[6] Montero S., I. C., Brimhall, G. H., Alpers, C. N., & Swayze, G. A. 2005. Characterization of waste rock associated with acid drainage at the Penn Mine, California, by ground-based visible to short-wave infrared reflectance spectroscopy assisted by digital mapping. Chemical Geology, 215(1-4 SPEC. ISS.): 453-472. https://doi.org/10.1016/j.chemgeo.2004.06.045.